Component Relaxation Processes within Elastomeric Polypropylene

Eric D. Carlson,[†] Gerald G. Fuller,*[,†] and Robert M. Waymouth*[,‡]

Department of Chemical Engineering and Department of Chemistry, Stanford University, Stanford, California 94305

Received August 4, 1998

ABSTRACT: The behavior of specific components of elastomeric polypropylene was directly observed in situ using a dynamic, infrared polarimetry technique. The elastomeric nature of ePP is presumed to arise from a multiblock structure of isotactic (iPP) and atactic (aPP) polypropylene blocks. Elastomeric polypropylene is a heterogeneous material in terms of tacticity that can be separated into fractions differing in tacticity. A series of samples were prepared in which one fraction was labeled with deuterium. Infrared dichroism measurements made at the C−^{2}H stretching vibration were used to follow the relaxation behavior of fractions of various tacticity. The samples were subjected to a series of step shear strain experiments at a variety of temperatures from the melt and into the crystalline region. By simultaneously measuring birefringence (which measures the bulk sample's local orientation) and IR dichroism (which measures the orientation dynamics of the deuterated fraction), it is possible to isolate the behavior of specific populations of chains. It was revealed that chains with the highest level of tacticity crystallize first, as is expected, and strongly influence the subsequent crystallization of the remaining chains. In addition, evidence of cocrystallization between the solvent fractions was observed.

Introduction

Elastomeric polypropylene belongs to an interesting class of single monomer thermoplastic elastomers and displays unique rheological behavior.[1] The material was first prepared by Natta, who interpreted its rubbery nature as the result of a multiblock structure of atactic strands tethered together by isotactic crystallites.[2−4] The level of stereoregularity within the polypropylene microstructure dictates its macroscopic physical behavior. Atactic polypropylene is stereoirregular and is an amorphous polymer. Syndiotactic and isotactic polypropylene are rigid materials with highly stereoregular structures able to form helices and pack into crystals. The stereoregularity of the polymer microstructures is generally determined by ^{13}C solution NMR measurements, from which the fraction of isotactic pentads, [mmmm], is used as an indicator of a sample's isotacticity. Elastomeric polypropylenes possess moderate [mmmm] values, and their behavior falls between the amorphous, atactic polymer and the rigid, isotactic polymer.

Elastomeric polypropylenes can be prepared with a variety of synthesis techniques, and both the microstructure and macroscopic behavior of these materials have been studied.[5−13] We have recently investigated the thermal and rheological behavior of elastomeric polypropylenes synthesized with metallocene catalysts derived from bis(2-phenylindenyl)zirconium dichlorides.[14−17] These catalysts were designed to produce blocks of atactic and isotactic stereosequences by having the ability interconvert between chiral and achiral coordination geometries.[18−20] Polypropylenes produced from these unbridged metallocene catalysts span a wide range of tacticities, from highly isotactic samples, to moderately isotactic, elastomeric samples, to highly atactic samples.

Recent studies have shown that elastomeric polypropylenes prepared from these unbridged metallocene catalysts are heterogeneous in terms of tacticity. The resulting polymer is a mixture of chains with varying degrees of tacticity. The parent polymer can be fractionated using a series of boiling solvents into components that differ in their [mmmm] values. Specifically, we have studied an elastomeric polypropylene (ePP, [mmmm] = 0.32) that fractionates into an ether-soluble fraction (ES, 36 wt %, [mmmm] = 0.18), a heptane-soluble fraction (HS, 43 wt %, [mmmm] = 0.33), and a heptane-insoluble fraction (HI, 21 wt %, [mmmm] = 0.51).

The role that composition plays in dictating the physical behavior is complex. Because of large microstructural differences between fractions, the individual fractions possess distinct thermal and rheological behavior. Thermal studies on the solvent fractions showed that the neat ES fraction demonstrated no crystallization while the neat HI fraction with its larger [mmmm] value exhibited a large amount of crystallization.[14] Although the HS fraction possesses the same average microstructure as the parent ePP sample measurements, we have shown that it exhibits significantly slower crystallization kinetics.[14] The fractions are rheologically distinct as well. The use of a dynamic birefringence experiment has allowed the recent study of the step shear strain response of these materials.[16,17] These studies showed that physical, crystalline cross-links in the ePP sample allow only a portion of the material to relax stress from an applied step shear deformation. This elastomeric network maintains some degree of chain orientations, revealed by an incomplete relaxation of the birefringence signal, until the deformation is reversed. It was shown that the neat ES fraction did not form an elastomeric network due to its low isotacticity, accounting for a large part of the relaxation seen in the parent sample. The neat HS fraction was shown to form some physical cross-links on its own, but despite its matching tacticity it was not as elastomeric as the parent ePP sample. The neat HI fraction was shown to

[†] Department of Chemical Engineering.
[‡] Department of Chemistry.
* To whom correspondence should be addressed.

10.1021/ma981236e CCC: $18.00
Published on Web 11/04/1999

behave as an elastic solid. Thus, in the parent sample the HI fraction is believed to be able to cocrystallize with fractions of lower isotacticity, providing a larger cross-link density within the ePP sample.

The current set of experiments seeks to directly observe the role each solvent fraction plays as it resides in the parent elastomer. To this end, a hydrogenated and a deuterated sample of ePP were prepared from an unbridged metallocene catalyst. After fractionation, these materials were reblended to create ePP analogue samples in which only one solvent fraction was labeled with deuterium. We follow the orientation of labeled chains with an dynamic infrared (IR) polarimetry experiment.[21−23] Similar to the dynamic birefringence experiment previously employed, IR polarimetry also tracks the orientation of polymer chains. With a laser tuned to the C−^{2}H stretching vibration, two optical signals are simultaneously monitored. First, a birefringence signal gives a measure of anisotropy in the orientation distribution of the bulk sample. At the same time a dichroism measurement indicates the amount of anisotropy in the orientation distribution of the deuterated fraction. To elucidate the role that each component plays in the establishment of the elastomeric network, the step shear strain response of the labeled elastomers was followed near the onset of crystallization.

Experimental Section

Materials. A hydrogenated elastomeric polypropylene sample (ePP) was prepared at Amoco Chemical Co. using an unbridged metallocene catalyst derived from bis(2-phenylindenyl)zirconium dichloride. The sample was fractionated by successive extraction with boiling diethyl ether and heptane under a nitrogen environment. The ePP system under investigation has 36% of an ether-soluble fraction (ES, [mmmm] = 0.18), 43% of a heptane-soluble fraction (HS, [mmmm] = 0.33), and 21% of a heptane-insoluble fraction (HI, [mmmm] = 0.51). An atactic polypropylene homopolymer was prepared with a metallocene catalyst to have an [mmmm] = 0.10, a M_w = 496 000, and an M_w/M_n = 2.7. Details of the preparation, purification, and characterization of all these samples have been reported previously.[14]

A deuterated elastomeric polypropylene for IR polarimetry experiments (d-ePP) was synthesized from bis(2-phenylindenyl)zirconium dichloride 20 °C and 75 psig. The methylaluminoxane (MAO) cocatalyst (Akzo type 4A, dried under vacuum at 60°) (0.76 g/mL) and bis(2phenylindenyl)zirconium dichloride catalyst precursor (0.004 g/mL) solutions were separately prepared in toluene. A 350 mL Parr reactor was flushed with argon at 20 °C, and 90 mL of toluene was added to the reactor. The reactor was pressurized to 45 psig with deuterated propylene and allowed to equilibrate for 30 min. Protonated propylene was then used to pressurize the reactor to 70 psig. An additional equilibration time of 30 min was allowed. The catalyst and catalyst precursor solutions were premixed and allowed to age for 30 min at room temperature. The catalyst solution was injected into the reactor with protonated propylene, and polymerization was conducted at 20 °C and 75 psig. After 45 min, the polymerization was terminated with the addition of 80 mL of methanol. Unreacted monomer was vented off, and the polypropylene was precipitated slowly into acidified methanol. Polymer was subsequently dried at 50 °C in vacuo. The yield for the polymerization under these conditions was approximately 7.8 g. Solution ^{13}C NMR measurements revealed that the bulk d-ePP sample has an [mmmm] = 0.33, and FT-Raman measurements indicated that the d-ePP sample is approximately 33% deuterated.

The d-ePP samples was fractionated in a Soxhlet extractor by successive extraction with ether and heptane under a nitrogen blanket at the boiling point of the solvent. Extracted polymer was recovered by slow precipitation into methanol and dried at 50 °C in vacuo. The d-ePP system under investigation has 35% of an ether-soluble fraction (dES), 46% of a heptane-soluble fraction (dHS), and 19% of a heptane-insoluble fraction (dHI). Systems of labeled ePPs were formed by blending a deuterated fraction in with fractions of the hydrogenated ePP (Figure 1). An ePP−dES blend was created by mixing 360 mg of the ether-soluble fraction of d-ePP with 430 mg of the heptane-soluble fraction of ePP and 210 mg of the heptane-insoluble fraction of ePP. An ePP−dHS blend was created by mixing 360 mg of the ether-soluble fraction of ePP with 430 mg of the heptane-soluble fraction of d-ePP and 210 mg of the heptane-insoluble fraction of ePP. An ePP−dHI blend was created by mixing 240 mg of the ether-soluble fraction of ePP with 287 mg of the heptane-soluble fraction of ePP and 140 mg of the heptane-insoluble fraction of d-ePP. All fractions were dissolved in boiling toluene and allowed to dissolve for 1 h. Blends were precipitated slowly into methanol and were subsequently dried at 50 °C in vacuo.[24]

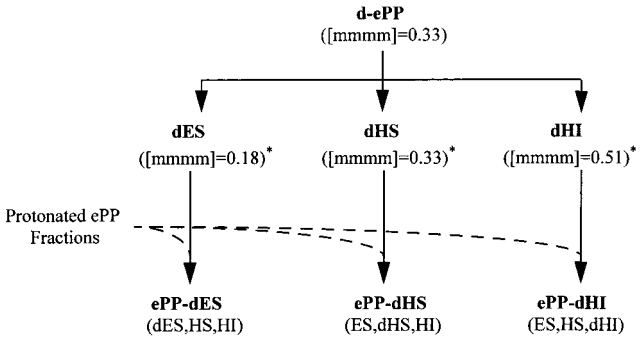

Figure 1. Isotopically labelled blends of ePP were prepared from deuterated and protonated solvent fractions. Isotactic content based on measurements of protonated samples.[24]

Isotacticity is reported in terms of the fraction of isotactic pentads [mmmm] as determined by ^{13}C NMR. Molecular weight characterization were carried out at Amoco Chemical Co. on a Waters 150C in trichlorobenzene at 145 °C and are referenced against polypropylene standards.

IR Polarimetry Measurements. The dynamic response to a large-amplitude step shearing flow was measured via an IR polarimetry experiment designed to monitor the time-dependent birefringence and dichroism resulting from polymer orientation.[21−23] Figure 1 contains the optical train for the IR polarimetry measurements. Deformation and flow are provided with a Linkam CSS 450 shearing apparatus; the flow direction is taken to be 0°. Monochromatic light is provided with an IR laser tuned to the C−^{2}H stretching vibration (2180−2195 cm^{-1}). The beam passes through a polarizer oriented at 0° followed by a photoelastic modulator (PEM) oriented at 45°. The polarization modulated beam then passes at normal incidence through a sample under parallel plate deformation, allowing the beam to pass along the shear gradient axis. Following the flow cell, the light impinges upon a beam splitter. Part of the light is reflected back through an analyzing polarizer oriented at 45° and is collected with detector 1. The rest of the beam passes through the beam splitter and into detector 2. The intensity observed at either detector is of the form

$$I = I_{dc} + I_{\omega}\sin(\omega t) + I_{2\omega}\cos(2\omega t) + ... \quad (1)$$

Lock-in amplifiers are used to demodulate the optical signals. A birefringence value is found using the intensity ratio from detector 1:

$$\frac{I^{(1)}_{\omega}}{I^{(1)}_{dc}} = 2J_1(A_{PEM})\sin(\delta'); \quad \delta' = \frac{2\pi d}{\lambda}\Delta n' \quad (2)$$

where δ' is the retardation, d is the sample thickness, λ is the

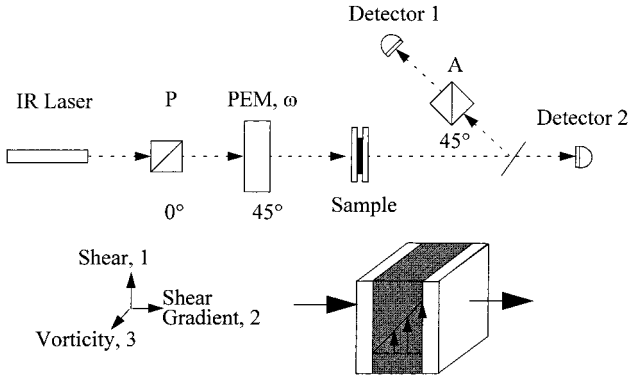

Figure 2. IR polarimetry optical train. Signal from detector 1 contains the birefringence information about the average orientation of thew bulk sample. Signal from detector 2 carries the dichroism data indicating the orientation of the ^{2}H-labeled fraction.

wavelength of light, and $\Delta n'$ is the birefringence. Similarly, a dichroism value is found using the intensity ratio from detector 2:

$$\frac{I^{(2)}_{2\omega}}{I^{(2)}_{\mathrm{dc}}} = 2J_2(A_{\mathrm{PEM}})\tanh(\partial'');\quad \partial'' = \frac{2\pi d}{\lambda}\Delta n'' \qquad (3)$$

where ∂'' is the attenuation and $\Delta n''$ is the dichroism. $J_1(A_{\mathrm{PEM}})$ and $J_2(A_{\mathrm{PEM}})$ are experimentally determined calibration constants using elements of known retardation and attenuation.

The samples were held in a Linkam shearing apparatus modified to contain a nitrogen environment. A rotational displacement voltage transducer was used to measure applied strains. Samples of thickness 200−500 μm were deformed in a parallel plate geometry with light propagating down the shear gradient axis; thus, birefringence and dichroism measurements indicate orientations in the 1−3 flow−vorticity plane. Polypropylene has a positive stress−optical coefficient, so a positive birefringence signal signifies polymer chains oriented in the flow direction.[25] Positive shear strain (100% shear strain at the point of measurement) was applied at time t_1 by a clockwise displacement of the bottom window. At time t_2 a negative deformation (−100% shear strain at the point of measurement) was applied by a counterclockwise displacement of the bottom window. All samples were prepared with the same thermal history. Samples were heated to 200 °C under nitrogen in the flow cell and held for 10 min to erase any thermal or strain history. Samples were then cooled at 20 °C/min to the experimental temperature of interest and held for 10 min to allow the sample to equilibrate.[26]

Results and Discussion

Using the IR polarimetry optical train described in the Experimental Section (Figure 2), the onset of network formation was examined by simultaneously monitoring the response of the average bulk sample and the response of the deuterated population of polymer chains to a step shear deformation. The intensity from detector 1 carries the birefringence information. Birefringence measurements have proven useful to probe the rheology of bulk elastomeric polypropylene systems.[16,17] In addition, with a laser tuned to the C−^{2}H stretching vibration, the intensity at detector 2 contains dichroism information indicating an anisotropy in the distribution of C−^{2}H bond orientations. To examine the onset of network formation, samples were cooled to a variety of temperatures from the melt (200 °C), held for 10 min, and then subjected to a step shear deformation (100% shear strain). Comparisons are drawn between samples made to have matching isotactic content. The inability to measure the isotactic content of the isolated deuterated fractions[24] combined with the process of blending and reprecipitation of samples may lead to some of the differences seen in these measurements which prohibit us from drawing quantitative comparison between samples.

Figures 3, 4, and 5 contain respectively the normalized birefringence and dichroism data on the ePP−dHI, ePP−dHS, and ePP−dES samples collected at a series of temperatures. Because we are interested in the amount of relaxation that occurs relative to the maximum orientation, values were normalized to the maximum value of the optical anisotropy following deformation. Each set of stacked graphs in each of the figures contains data collected at a different temperature. The top graph in each set displays the birefringence data which represent the time-dependent, average orientation of the bulk sample. The bottom graph in each set contains the dichroism data which show the time-dependent orientation of the deuterated fraction. Data are presented from a series of experiments carried out at progressively lower temperatures.

At 200 °C, both birefringence and dichroism signals for all three samples were able to relax to zero from a reversed step strain experiment showing that the bulk sample and each of the fractions were able to recover to an isotropic state between deformations at this temperature. As the temperature was decreased, full relaxation of both the birefringence and dichroism signal was observed for experiments carried out at temperatures $T \geq 105$ °C. Below 105 °C, the various fractions show a variety of behavior. Figure 3 shows that at 100 °C the ePP−dHI dichroism signal did not relax to zero but instead revealed a relaxation plateau following the initial step deformation. The ratio of the residual birefringence to the residual dichroism in this sample is about 1:2. The higher residual dichroism shows that after deformation there are more semipermanent orientations and stress within the labeled HI fraction than the bulk sample. In contrast, the dichroism of the dHS and dES fractions relaxes to essentially zero at 105 °C, showing that these fractions were not participating in the network (Figures 4 and 5).

At lower experimental temperatures the birefringence develops a strong upturn which will be addressed below, and differences in the dichroism signals of the three fractions become exaggerated. At 95 °C the data from the ePP−dHI sample show that neither the birefringence nor the dichroism relaxed back to zero following the initial deformation (Figure 3), and the level of the dHI relaxation plateau continued to increase as the temperature was decreased. At 84 °C the dHI fraction essentially responded as an elastic solid, with very little relaxation on the time scale of the experiment. Data from the ePP−dHS sample suggest that elastomeric behavior is established in both the bulk and the dHS fraction. Figure 4 shows that below 105 °C the there is a slight residual birefringence and residual dichroism following the initial deformation; as the temperature was decreased, both the residual birefringence and the dichroism signals increase in intensity. The dichroism data in Figure 5 show that the dES fraction was able to completely relax its flow-imposed orientation under the temperature conditions investigated, while the birefringence indicates the sample established an elastomeric network below 105 °C.

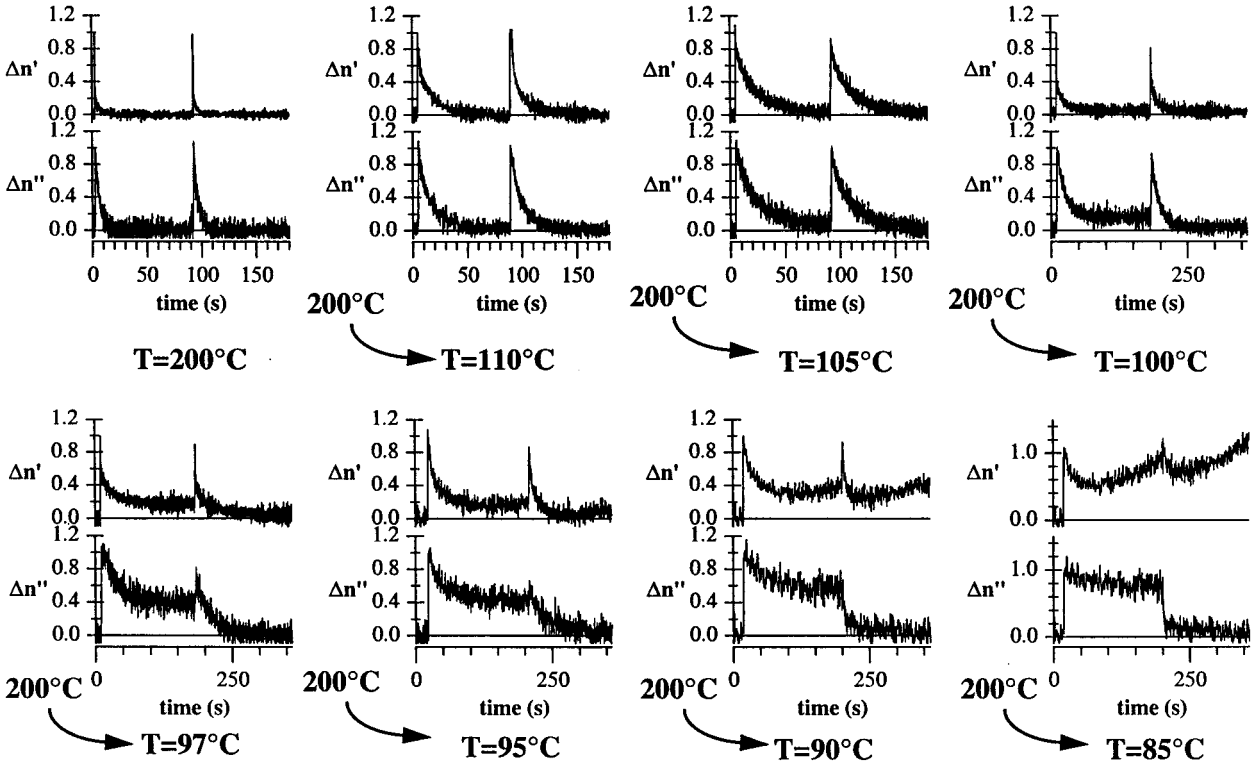

Figure 3. IR polarimetry results of ePP−dHI subjected to reversed step shear strain. The top graph in each set depicts the birefringence response as a function of time. The bottom graph in each set depicts the dichroism associated with the ^{2}H-labeled HI fraction as a function of time.

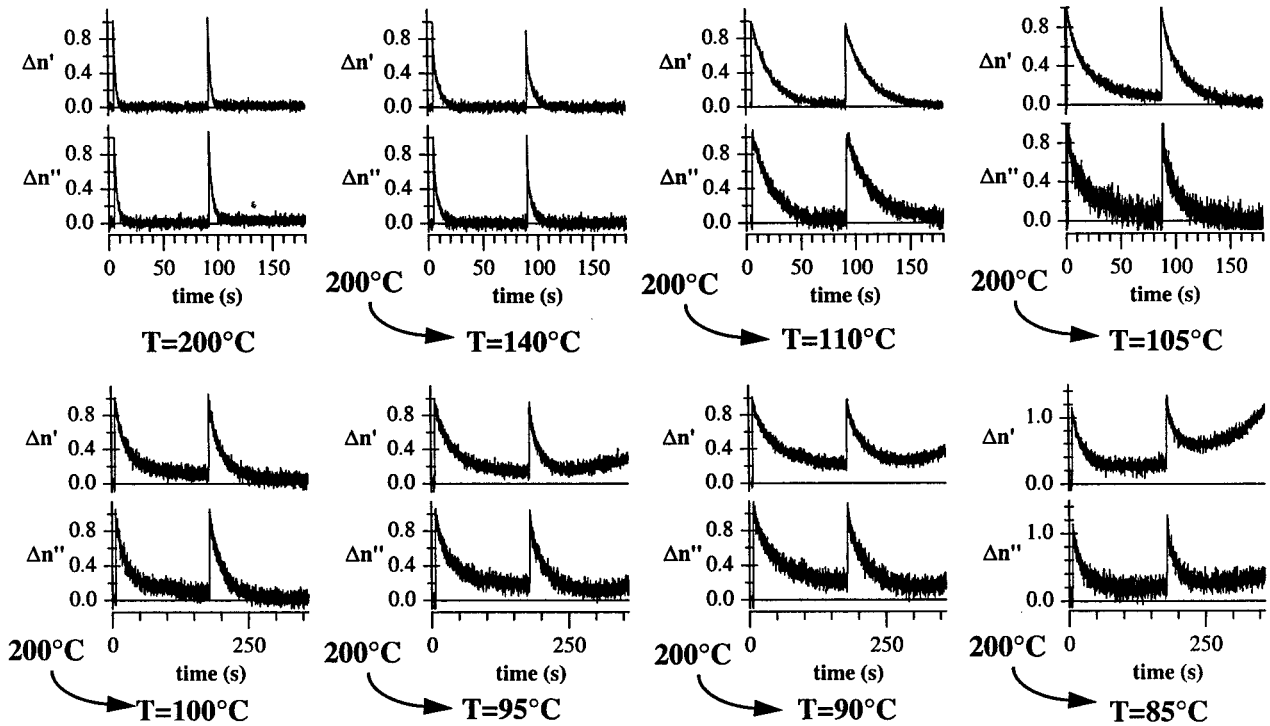

Figure 4. IR polarimetry results of ePP−dHS subjected to reversed step shear strain. The top graph in each set depicts the birefringence response as a function of time. The bottom graph in each set depicts the dichroism associated with the ^{2}H-labeled HS fraction as a function of time.

Figure 6 plots the level of the relaxation plateau for the dichroism and birefringence signals of the ePP−dHI sample against the temperature.[27] The data show that elastomeric behavior is observed in the dHI fraction prior to the bulk, demonstrating that the HI fraction crystallizes before most of the bulk sample and is responsible for establishing the elastomeric network. Data on the ePP−dHS and ePP−dES samples are consistent with this result, as shown in Figures 7 and 8 which plot the temperature dependence of the plateau in the birefringence and the dichroism of the ePP−dHS and ePP−dES samples, respectively. These graphs show

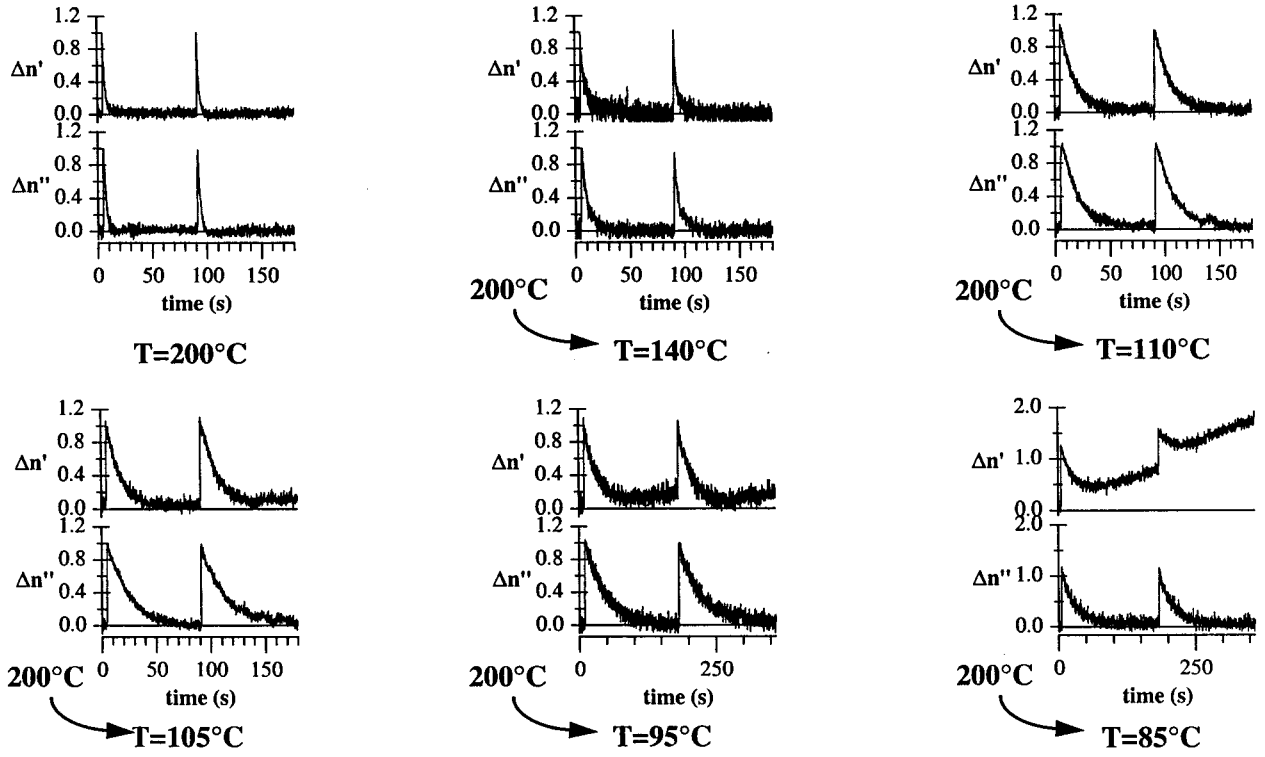

Figure 5. IR polarimetry results of ePP−dES subjected to reversed step shear strain. The top graph in each set depicts the birefringence response as a function of time. The bottom graph in each set depicts the dichroism associated with the ^{2}H-labeled ES fraction as a function of time.

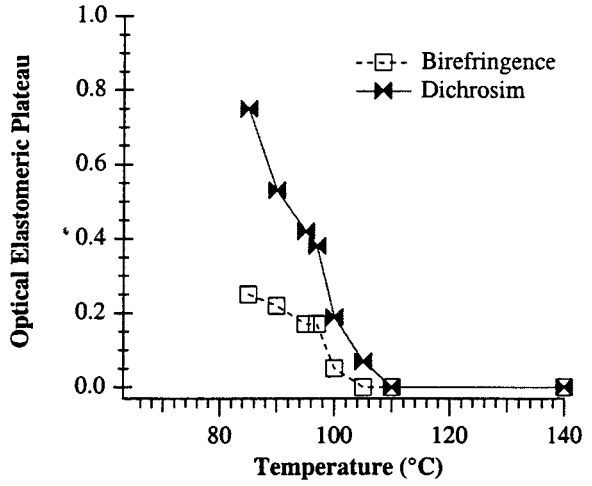

Figure 6. ePP−dHI elastomeric plateau: relaxation plateau vs temperature.

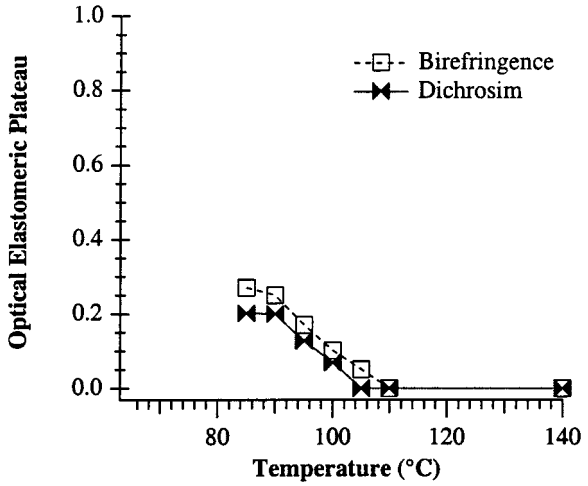

Figure 7. ePP−dHS elastomeric plateau: relaxation plateau vs temperature.

that the bulk elastomeric network is established within the HI and the HS fractions and that the ES fraction does not contribute to the elastomeric behavior of the ePP sample under these conditions.

Overall, the birefringence data from the three labeled samples, ePP−dHI, ePP−dHS, and ePP−dES, show that these samples behave qualitatively the same, with elastomeric behavior emerging at experiments conducted between 97 and 105 °C. Differences between the birefringence data from the three samples are due to the difficulty in preparing exact replicas through mixing and precipitation of different samples.[24] Thus, while the bulk responses, denoted by the birefringence data, are not quantitatively the same from sample to sample, the trends are consistent, and we are able to draw comparison between the behavior of the various solvent fractions. In addition, the birefringence signals at temperatures below 105 °C show interesting trends that should be addressed. Data taken at temperatures below approximately 95 °C showed a steady increase in the birefringence signal superimposed over the step relaxation response of all three ePP samples. Near 95 °C the growth in birefringence for all three samples was small and did not begin until after the reversed step deformation was applied. This rise in birefringence became much more prominent at lower temperatures and at 85 °C was apparent even after the initial deformation. We attribute this increase in the birefringence signal to crystallization taking place in the bulk in the shear direction. In the absence of flow, the birefringence remained zero even after very long times (t > 5000 s) for all three samples, indicating that a quiescent sample crystallizes isotropically. These results suggest that the initial physical crystalline cross-links form semiperma-

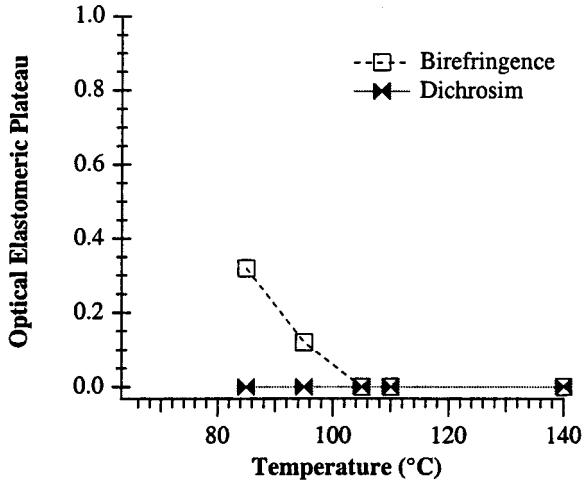

Figure 8. ePP−dES elastomeric plateau: relaxation plateau vs temperature.

nent orientations in the strained material that are able to strongly influence subsequent crystallization in the bulk sample. While these experiments indicate a preferred orientation of crystallized chains, they do not offer any evidence for or against enhanced crystallization due to flow. Prior step deformation experiments on aged elastomeric polypropylenes at room temperature have shown that an irreversible anisotropy can be induced through the application of the large shear ($\gamma > 50\%$).[16] Although flow-induced crystallization has been studied in isotactic polypropylene,[28−31] there has been limited work on the phenomenon within elastomeric polypropylene.[32] Further studies are planned to determine the effect of flow on the amount of crystallization in these elastomeric polypropylenes.

Surprisingly, the dichroism measurements were unable to capture most of this linear increase in optical anisotropy. Only the ePP−dHS sample showed any linear rise in the dichroism signal, and the rise was significantly smaller than was seen in the birefringence. While the increase in the ePP−dHS dichroism data does suggest that the deuterated HS fraction participated in any oriented crystallization process in these experiments, it is a concern that we were unable to fully attribute the rise in the birefringence to any of our labeled fractions through the dichroism measurements. The disparity between the rise birefringence and dichroism signals may have resulted from several factors. First, as mentioned above, the difficulty in preparing replica samples through mixing and precipitation of different fractions is a likely source of inconsistency. Variations in the isotactic content will result in different crystallization kinetics. More deuterated material needs to be synthesized and fractionated to allow for careful [mmmm] measurements on the isolated deuterium-labeled fractions. Second, the deuterated population of isotactic chains may represent the portion of isotactic chains with the slowest crystallization kinetics. A measurable difference in kinetics due to isotopic labeling seems unlikely given the degree of isotopic labeling in these systems (d-ePP was approximately 33% deuterated); however, Mezghani and Phillips have reported that perdeuterated isotactic polypropylene crystallizes at a lower temperature than the hydrogenated polymer.[33] Further experiments are necessary to rigorously study the kinetic effect on crystallization of selective deuteration. Finally, differences in the measured birefringence and dichroism can arise from form or scattering effects. Onuki and Doi have shown that the form dichroism appears at a higher order in wavenumber than the form birefringence;[26] thus, the dichroism measurement may be much less sensitive to form effects at the wavelength used in the present study (4600 μm). However, we have found no independent supporting evidence of structures that would cause form scattering in these samples. In the visible spectrum these samples are not turbid and do not scatter light anisotropically. Optical microscopy does not reveal any macroscopic spherulitic structures, TEM has been unable to resolve any mesoscopic structure on the order of 100−500 nm, and crystalline lamellar structures are too small (15 nm) to generate appreciable scattering.

Conclusions

The IR polarimetry data have demonstrated clear differences between the in situ behavior of various fractions of elastomeric polypropylene. The parent ePP system has a T_m of 142 °C as determined by DSC measurements and exhibits broad melting indicative of a heterogeneity of crystalline species.[14] The IR polarimetry results showed that the HI fraction becomes elastomeric before most of the bulk sample and that the ES fraction does not crystallize or contribute to the elastomeric network in these ePP systems. While it has been shown that for neat fractions the T_c increases with increasing [mmmm],[14,35,36] these data offer the first evidence of a separation in crystallization kinetics between elastomeric polymer fractions in situ. In addition, these data also offer evidence of cocrystallization within between the HS and the HI fractions. We have previously shown that the neat HS fraction crystallizes only at very long times with extremely slow kinetics. When blended in with the other fractions, the HS fraction is evidently able to crystallize on the time scales of the IR polarimetry experiments and to participate in the elastomeric network at these temperatures. This suggests that isotactic segments within the HS fraction that are kinetically unable to crystallize on their own can cocrystallize with the HI fraction. Cocrystallization of stereoblock polypropylenes is an idea supported by others who have studied elastomeric polypropylenes.[8,37,38] These experiments offer no evidence of physical crosslinks formed from the ES fraction of this polymer under these conditions. However, preliminary results from current solid-state ^{2}H NMR studies have shown that a portion of the ES chains are rigid and immobile in room-temperature aged, elastomeric samples. Thus, the appropriate thermal conditions may allow segments within the ES fraction to cocrystallize with the higher [mmmm] species present in the ePP sample.

Finally, these polarimetry data suggest that flow can affect the orientation of subsequent crystallization. A growth in overall sample orientation is measured following flow in these ePP samples. Further studies are planned to pursue the effect of flow on the subsequent crystallization of elastomeric polypropylene.

Acknowledgment. E.D.C. acknowledges the National Science Foundation for Graduate Fellowship support. G.G.F. acknowledges the National Science Foundation (NSF DMR 9522642-001) for financial support. R.M.W. acknowledges Amoco Chemical Company, NSF (NSF DMR 9528636-002), and the Center for Polymeric and Interfacial Macromolecular Assemblies

(CPIMA) for financial support. We also thank Amoco Chemical Company for providing the elastomeric sample and the molecular weight data. Finally, we thank Dr. Dave Ylitalo for initial discussions involving labeled fractions and S. Lin for her help in the preparation of the deuterated elastomeric polypropylenes.

References and Notes

(1) *Thermoplastic Elastomers: A Comprehensive Review*; Legge, N. R., Holden, G., Schroeder, H. E., Eds.; Hanser Verlag: New York, 1988.
(2) Natta, G.; Mazzanti, G.; Crepsi, G.; Moraglio, G. *Chim. Ind. (Milan)* **1957**, *39*, 275−283.
(3) Natta, G. *J. Polym. Sci.* **1959**, *34*, 531−549.
(4) Natta, G.; Crespi, G. U.S. Patent 3,175,999, 1965.
(5) Ziegler, K.; Holzkamp, H.; Martin, H. *Angew. Chem.* **1955**, *67*, 541−547.
(6) Ziegler, K. *Angew. Chem.* **1964**, *76*, 545.
(7) Collette, J. W.; Tullock, C. W., E. I. du Pont de Nemours, U.S. Patent 4,335,225, 1982.
(8) Collette, J. W.; Tullock, C. W.; MacDonald, R. N.; Buck, W. H.; Su, A. C. L.; Harrel, J. R.; Mulhaupt, R.; Anderson, B. C *Macromolecules* **1989**, *22*, 3851−3858.
(9) Collette, J. W.; Overnall, D. W.; Buck, W. H.; Ferguson, R. C. *Macromolecules* **1989**, *22*, 3858−3866.
(10) Llinas, G. H.; Dong, S.-H.; Mallin, D. T.; Rausch, M. D.; Lin, Y.-G.; Winter, H. H.; Chien, J. C. W. *Macromolecules* **1992**, *25*, 1242−1253.
(11) Mallin, D. T.; Rausch, M. D.; Lin, Y.-G.; Dong, S.; Chien, J. C. W. *J. Am. Chem. Soc.* **1990**, *112*, 2030−2031.
(12) Chien, J. C. W.; Llinas, G. H.; Rausch, M. D.; Lin, G. Y.; Winter, H. H. *J. Am. Chem. Soc.* **1991**, *113*, 8569−8570.
(13) Lin, Y.-G.; Mallin, D. T.; Chien, J. C. W.; Winter, H. H. *Macromolecules* **1991**, *24*, 850−854.
(14) Carlson, E. D.; Krejchi, M. T.; Shah, C. D.; Terakawa, T.; Waymouth, R. M.; Fuller, G. G. *Macromolecules* **1998**, *31*, 5343−5351.
(15) Hu, Y.; Krejchi, M. T.; Shah, C. D.; Myers, C. M.; Waymouth, R. M. *Macromolecules* **1998**, *31*, 6908−6916.
(16) Carlson, E. D.; Fuller, G. G.; Waymouth, R. M. *Macromolecules* **1999**, *32*, 8094−8099.
(17) Hu, Y.; Carlson, E. D.; Fuller, G. G.; Waymouth, R. M. *Macromolecules* **1999**, *32*, 3334−3340.
(18) Coates, G. W.; Waymouth, R. M. *Science* **1995**, *267*, 217−219.
(19) Hauptman, E.; Waymouth, R. M.; Ziller, *J. W. J. Am. Chem. Soc.* **1995**, *117*, 11586−11587.
(20) Kravchenko, R.; Masood, A.; Waymouth, R. M. *Organometallics* **1997**, *16*, 3635−3639.
(21) Kornfield, J. A.; Fuller, G. G.; Pearson, D. S. *Macromolecules* **1991**, *24*, 5429−5441.
(22) Ylitalo, C. M.; Kornfield, J. A.; Fuller, G. G.; Pearson, D. S. *Macromolecules* **1991**, *24*, 749−758.
(23) Zawada, J. A.; Ylitalo, C. M.; Fuller, G. G.; Colby, R. H.; Long, T. E. *Macromolecules* **1992**, *25*, 2896−2902.
(24) It should be noted that [mmmm] measurements were not performed on the isolated, deuterated fractions of the elastomeric sample. Solvent fractionation resulted in almost equivalent percentages of the ether-soluble, heptane-soluble, and heptane-insoluble fractions as the protonated material (see ref 14); thus for the purposes of this study they were considered to have equivalent isotactic content. While we do not expect deuterium to have a drastic effect on the polymerization kinetics, studies of the effect of isotopic labeling on polymerization are underway.
(25) Janeschitz-Kriegl, H. *Polymer Melt Rheology and Flow Birefringence*; Springer-Verlag: Berlin, 1983.
(26) An independent thermocouple was used to measure the sample temperature near the aperture where the measurements were taken. The sample temperature was found to vary from the reading in the Linkam software for different sample thicknesses.
(27) The plateau vaue of the birefringence data was found by subtracting the linear increase in the low-temperature birefringence data from the overall signal.
(28) Varga, J.; Kargerkocsis, J. *J. Appl. Polym. Sci.* **1996**, *34*, 657−670.
(29) Vleeshouwers, S.; Meijer, H. E. H. *Rheol. Acta* **1996**, *35*, 391−399.
(30) Anderson, P. G. *Polym. Prepr.* **1975**, *16*, 475−480.
(31) Kumaraswamy, G.; Verma, R. K.; Kornfield, J. A. *Rev. Sci. Instrum.* **1999**, *70*, 2097−2104.
(32) Canevarolo, S. V.; De Candia, F. *J. Appl. Polym. Sci.* **1996**, *61*, 217−220.
(33) Mezghani, K.; Phillips, P. J. *Macromolecules* **1994**, *27*, 6145−6146.
(34) Onuki, A.; Doi, M. *J. Chem. Phys.* **1986**, *85*, 1190−1197.
(35) Janimak, J. J.; Cheng, S. Z. D.; Zhang, A. Q.; Hsieh, E. T. *Polymer* **1992**, *33*, 728−735.
(36) Paukkeri, R.; Lehtinen, A. *Polymer* **1993**, *34*, 4083−4088.
(37) Canevarolo, S. V.; De Candia, F. *J. Appl. Polym. Sci.* **1994**, *54*, 2013−2021.
(38) Canevarolo, S. V.; De Candia, F.; Russo, R. *J. Appl. Polym. Sci.* **1995**, *55*, 387−392.

MA981236E